

# Developing a New Tool for Modeling the Topology of Zero Sets of Bivariate Pentanomials: A Near-Circuit Case

Vaishali Miriyagalla

July 28, 2023

## Abstract

There are many practical applications for solving the zero sets of polynomials but they are time-consuming to solve, considered to be NP hard.  $\mathcal{A}$ -discriminants are a tool to group sets of coefficients with zero sets of the same topology. For near circuits (polynomials with  $n + 3$  terms, where  $n$  is the number of variables), the  $\mathcal{A}$ -discriminant can be reduced to two dimensions, making this grouping easier. This paper will focus on the implementation of a MATLAB program that can help model the isotopy types of zero sets of bivariate pentanomials.

## 1 Background

### 1.1 Supports and Near Circuits [FNR17]

**Definition 1.1.** (Support of a polynomial) Given the polynomial, where the  $c_i$  are the coefficients of each monomial term and the  $a_{i,j}$  are the exponents of the  $j$ th variable of the  $i$ th monomial.

$$f = \sum_{i=0}^{n+k} \left( c_i \prod_{j=1}^n x_j^{a_{i,j}} \right)$$

Then the *support* of  $f$  is the set of exponent vectors. It is the  $n \times (n+k)$  matrix  $\mathcal{A} = \begin{bmatrix} a_{1,1} & \cdot & \cdot & \cdot & a_{n+k,1} \\ \cdot & \cdot & \cdot & \cdot & \cdot \\ \cdot & \cdot & \cdot & \cdot & \cdot \\ \cdot & \cdot & \cdot & \cdot & \cdot \\ a_{1,n} & \cdot & \cdot & \cdot & a_{n+k,n} \end{bmatrix}$

Because each column of  $\mathcal{A}$  represents a monomial term of  $f$ , each column is distinct.

**Definition 1.2.** (Near Circuit) A polynomial  $f$  with support  $\mathcal{A}$  a *near circuit* polynomial iff  $\mathcal{A}$  has cardinality  $n + 3$  (i.e.  $\mathcal{A}$  has  $n + 3$  columns and distinct rows).<sup>1</sup>

For any given near-circuit polynomial, there are many different coefficient combinations that will produce positive real zero sets. Descartes Rule of Signs states that the number of real roots of a univariate polynomial is less than or equal to the number of sign changes between any  $c_i$  and  $c_{i+1}$ . Sign changes impact the number of positive real roots in the univariate case. This understanding can be expanded to  $n > 1$  cases. For example, if all signs of the polynomial's coefficients are the same, it is not possible to have any roots. The number of sign changes may alter the number of connected components (ie. pieces or hypersurfaces) that make up the zero set.

Going beyond just sign changes, for a fixed set of sign changes, the magnitude of the coefficients can change the topology of the zero set. In order to get a better understanding of these topological changes, we look at  $\mathcal{A}$ -discriminants. Recall the discriminant for quadratics from high school Algebra (for  $ax^2 + bx + c$ , the discriminant is  $b^2 - 4ac$ ): if  $b^2 - 4ac < 0$ , no roots; if  $b^2 - 4ac > 0$ , two roots; if  $b^2 - 4ac = 0$ , one root.

<sup>1</sup>Near circuit polynomials are sparse polynomials because they can have very high degrees but comparatively few terms.

## 1.2 $\mathcal{A}$ -discriminants and Topology of Zero sets

Similar to the quadratic discriminant,  $\mathcal{A}$ -discriminants are formulas dependent on the coefficients of the polynomial. Each unique support has a unique  $\mathcal{A}$ -discriminant formula.

**Definition 1.3.** The  $\mathcal{A}$ -discriminant is a polynomial in coefficients of  $f$  (as defined above) vanishing when  $f$  has a singular zero set.

**Definition 1.4.** The  $\mathcal{A}$ -discriminant variety is the closure of the set of coefficients that give the polynomial  $f$  a degenerate zero set.

The  $\mathcal{A}$ -discriminant variety is also used as a curve that represents the precise coefficient combinations that result in topological changes in the zero set. Unfortunately, these  $\mathcal{A}$ -discriminant varieties become increasingly unrealistic to numerically solve once the exponent vectors are more complex than a quadratic or cubic.

Near circuits provide a special case where the  $\mathcal{A}$ -discriminant is always represented in two dimensional space. We call this simplified version the *reduced*  $\mathcal{A}$ -discriminant. This allows us to model the changes of  $n+3$  coefficients with just a flat plane regardless of  $n$  (number of variables) or  $d$  (highest degree). Consequently, instead of trying to write down the formula for the explicit  $\mathcal{A}$ -discriminant variety, we parametrize the curve in two variables. See Section 2 for this parametrization and an example.

The  $\mathcal{A}$ -discriminant variety is made up of *signed contours*.

**Definition 1.5.** A *signed contour* is the closure of the set of coefficients  $c = [c_1, \dots, c_{n+3}]$  with sign changes specified by  $s = [s_1, \dots, s_{n+2}]$ , where  $s_i \in \{0, 1\}$ , that give the polynomial a degenerate zero set.

Looking at signed reduced contours is easier than looking at the reduced  $\mathcal{A}$ -discriminant variety because it allows us to work in an even smaller set of cases.

We can think of each signed contour as a portion of the parametrized  $\mathcal{A}$ -discriminant that lies between two points that shoot off to infinity (infinite singularities).

Each signed contour separates the reduced coefficient space into distinct regions called *chambers*.

**Definition 1.6.** An *inner* chamber is a chamber that is entirely bound by a sign contour. An *outer* chamber is a chamber that has a portion that extends to infinity.

Outer chambers are more common than inner chambers because most signed contours do not loop back across themselves (since each signed contour exists between two points that approach infinity). Furthermore, the set of coefficients that map to inner chambers tend to have zero sets with unique properties that are more difficult to model.

**Proposition 1.1.** All coefficient combinations whose  $\mathcal{A}$ -discriminant lies in one chamber are ambiently isotopic. [Mil69] [Har80]

In simpler terms, if  $f$  and  $g$  are  $n+3$  polynomials with support  $\mathcal{A}$  also have  $\mathcal{A}$ -discriminants that lie in the same chamber, it is possible to transform the zero set of  $f$  into the zero set of  $g$  without tearing or fusing.

**Lemma 1.1.** For  $n = 2$ , there are at most 3 possible chambers for any given sign combination.

Lemma 1.1 quickly follows from the following proposition. Since there is at most 2 cusps within one signed contour, there are at most one inner chamber and two outer chambers, so a maximum of three chambers.

**Proposition 1.2.** For near-circuits, there are at most  $n$  cusps within one signed contour. [RR17]

If one were to know the isotopy type of each chamber for support  $\mathcal{A}$ , one could determine the isotopy type of any polynomial with that support: simply map the coefficient vector down to a two coordinate point. And visually it becomes quite apparent which chamber that point lies in. This would thoroughly simplify and speed up the process of approximating zero sets for near circuits.

Still this simplification has two nontrivial components. Since we cannot explicitly solve for the  $\mathcal{A}$ -discriminant and used a parametrization for the  $\mathcal{A}$ -discriminant variety, algorithmically determining the chamber of one polynomial is difficult. Even though we may be able to literally see which chamber the point lies in, the inequality that algorithmically determines the chamber of a coordinate is an additional complication. Furthermore, determining the isotopy type within each chamber becomes increasingly nuanced as  $n$  gets larger. For  $n = 2$  Viro Diagrams model well in outer chambers but no longer work in inner chambers of if  $n \geq 3$ .

### 1.3 Goal

This paper will look at automating the  $\mathcal{A}$ -discriminant approach to modeling the isotopy types for zero sets of bivariate pentanomials. Specifically, it seeks to implement the following for any  $n = 2$  near-circuit:

1. Draw the  $\mathcal{A}$ -discriminant variety for the given support.
2. Find which signed contours may have inner chambers.
3. Determine the isotopy types within each outer chamber using Triangulation and Viro Patchworking Diagrams.
4. Continue improving approximations for signed contours to move toward reliably determining the chamber a given set of coefficients within the  $\mathcal{A}$ -discriminant space.

## 2 Parametrize $\mathcal{A}$ -discriminant Variety: Horn-Kapranov Uniformization [Kap91]

For any  $n \times (n + 3)$  support  $\mathcal{A}$ , let  $\hat{\mathcal{A}}$  be the  $(n + 1) \times (n + 3)$  matrix with first row  $[1, \dots, 1]$  and bottom  $n$  rows forming  $\mathcal{A}$ . Then let  $\mathcal{B}$  be a  $(n + 3) \times 2$  matrix<sup>2</sup> whose columns form a basis for the right nullspace of  $\hat{\mathcal{A}}$ . Let  $\mathcal{B}^\top$  be the transpose of  $\mathcal{B}$ . Let  $\lambda \in \mathbb{P}_{\mathbb{C}}^1$  be the variable of parametrization where  $\lambda = [\lambda_1 : \lambda_2]^3$ .

**Proposition 2.1.** Then  $\log |\lambda \cdot \mathcal{B}^\top| \cdot \mathcal{B}$  yields a  $2 \times (n + 3)$  matrix where the two rows give the parametrization of the  $\mathcal{A}$ -discriminant variety in 2D space.

**2.1 Example:**  $f(x, y) = c_1 + c_2x + c_3y + c_4x^4y + c_5xy^4$

$$\text{Support } \mathcal{A} = \begin{bmatrix} 0 & 1 & 0 & 4 & 1 \\ 0 & 0 & 1 & 1 & 4 \end{bmatrix}, \text{ so } \hat{\mathcal{A}} = \begin{bmatrix} 1 & 1 & 1 & 1 & 1 \\ 0 & 1 & 0 & 4 & 1 \\ 0 & 0 & 1 & 1 & 4 \end{bmatrix}.$$

The resulting  $\mathcal{A}$ -discriminant variety, specified by  $\log |\lambda \cdot \mathcal{B}^\top| \cdot \mathcal{B}$  is depicted in Figure 1a, but as mentioned, it is more valuable to look at signed reduced contours. One particularly interesting signed contour, specified in Figure 1b, has the sign pattern of  $++-+-$  (or  $--+--$ ). It has an inner chamber.

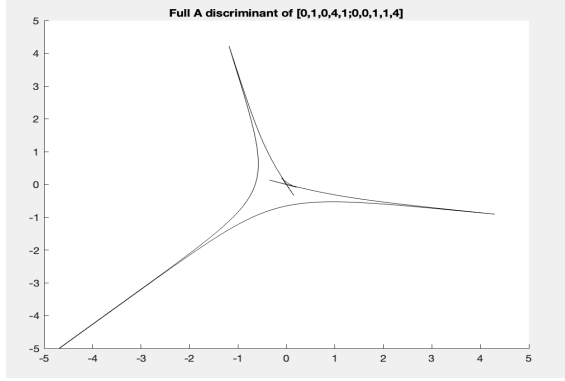
There are three chambers present in the signed contour in 1b. Call the two outer chambers in the bottom left and top right, chambers  $s_1$  and  $s_3$  respectively and the inner chamber chamber  $s_2$ .

The isotopy types of the zero sets within each of these chambers is depicted in Figure 2.

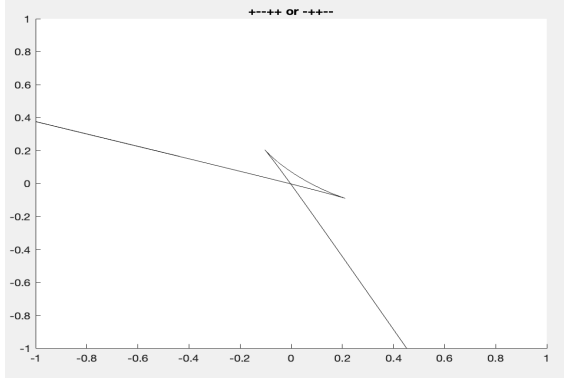
These isotopy types were found by solving for the zero sets of polynomials that had coefficients that mapped to each of these three chambers. This process is comparatively slow and *NP Hard*. The goal is to move beyond this kind of brute force method and toward a simpler process of finding the isotopy types of zero sets. The current modeling process for finding isotopy types only works on outer chambers, so first we need to identify and flag signed contours that may have inner chambers.

<sup>2</sup>2 columns because  $(n + 3) - n = 2$

<sup>3</sup>it is convenient to use  $\lambda = [\cos t, \sin t]$ , where  $t \in [-\frac{\pi}{2}, \frac{\pi}{2}]$

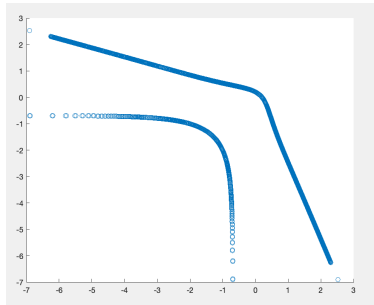


(a) full  $\mathcal{A}$ -discriminant variety of  $f$

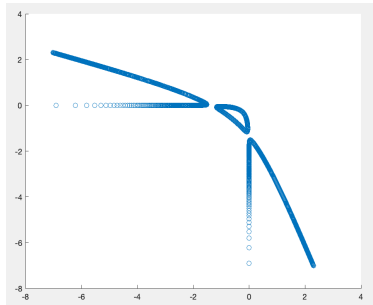


(b) signed contour:  $+-+-$  (or  $-+ -+$ )

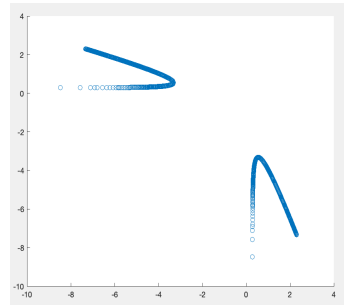
Figure 1: Support =  $\begin{bmatrix} 0 & 1 & 0 & 4 & 1 \\ 0 & 0 & 1 & 1 & 4 \end{bmatrix}$



(a)  $s_1$



(b)  $s_2$



(c)  $s_3$

Figure 2: Isotopy types within chambers of signed contour  $+-+-$  (or  $-+ -+$ )

### 3 Detecting Inner Chambers in Signed Contours

This paper primarily employs Triangulations and Viro's Patchworking to determine isotopy types, but these techniques are only reliable in outer chambers. Before employing these tools of approximation, we should eliminate signed contours that may have an inner chamber.

Trivially, inner chambers can only arise if there are at least two cusps within one signed contour. And by Proposition 1.2 (there are at most  $n$  cusps within on signed chamber for near-circuit supports) [RR17], the bivariate case means that inner chambers can only arise if there are two cusps.

Importantly, having two cusps does not necessarily create an inner chamber. Still, in order to eliminate the possibility of an inner chamber, one must find cusps. The following outlines the steps for finding cusps:

1. Find the derivatives ( $\frac{dx}{dt}$  and  $\frac{dy}{dt}$ ) of each signed contour of the parametrized  $\mathcal{A}$ -discriminant variety.
2. Find where both  $\frac{dx}{dt} = 0$  and  $\frac{dy}{dt} = 0$ ; then solve for  $x$  and  $y$ .

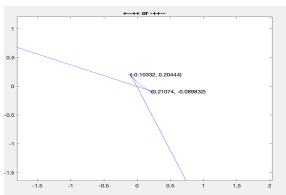


Figure 3: Two Cusps in  $+- -+ +$

Figure 3 shows the cusps in  $+- -+ +$  of  $\mathcal{A} = \begin{bmatrix} 0 & 1 & 0 & 4 & 1 \\ 0 & 0 & 1 & 1 & 4 \end{bmatrix}$ .

With a method to isolate sign contours with two cusps, we can turn to determining the isotopy types of outer chambers.

## 4 Isotopy Types of Outer Chambers: Triangulations and Viro's Patchworking Diagrams

The basic steps of this technique are as follows [Vir00]:

1. Plot the exponent vectors of the polynomial (columns of the support) as points. Draw a convex polytope using these points.
2. Label each point with the corresponding signs of the polynomial.
3. Identify edges with vertices of opposite signs. Draw outer normals from these edges and connect these edges inside the convex polytope. The resulting drawing gives the isotopy type of the zero set.

Figure 4 gives an example using a simpler support:  $\mathcal{A} = \begin{bmatrix} 1 & 0 & 1 \\ 0 & 1 & 1 \end{bmatrix}$ .

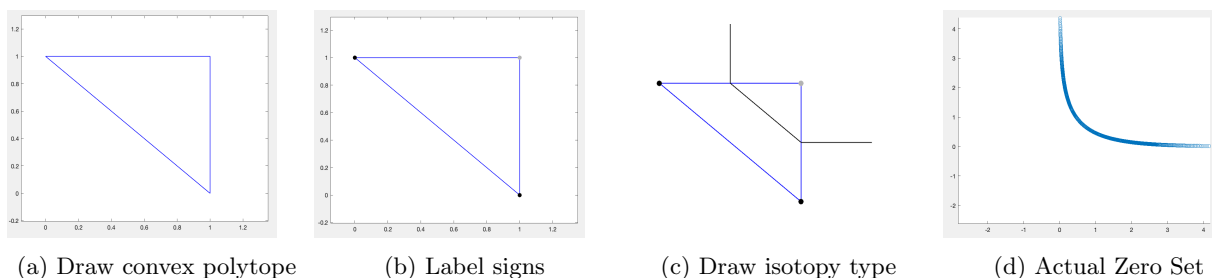


Figure 4: Isotopy type of Support  $\mathcal{A} = \begin{bmatrix} 1 & 0 & 1 \\ 0 & 1 & 1 \end{bmatrix}$ .

### 4.1 Triangulations with Five Points

This process can be extended to the bivariate near-circuit case but recall it can only be applied for outer chambers. Bivariate near-circuits have five terms and thus five exponent vectors. Again, we will plot the columns of the support as points and draw a convex polytope. However this time, we have five vertices and the resulting convex polytope does not give a triangulation. Rather there are many possible triangulations that can arise. These triangulations will result in different isotopy types. Naturally, different outer chambers of the coefficient space have different triangulations. In order to determine the different triangulations in these outer chambers, we need to use a *Lifted Convex Hull*.

We vertically concatenate a third row to the support to form our *lifted support* in three dimensions. This third row is defined by  $-\log |c|$ , where  $c = [c_1 \ c_2 \ c_3 \ c_4 \ c_5]$ , the given coefficient vector. Then we compute the convex hull of the lifted support. The faces of this lifted convex hull are triangles and we identify which triangle faces have positive inner normals (or negative outer normals). These triangles will form the triangulation used for the outer chamber that  $c$  lies in.

It is important to note that different coefficient vectors will result in different convex hulls providing different triangulations. When finding a coefficient vector to represent a chamber, it is most reliable and effective to use a coefficient vector that lies far out in an outer chamber, not one that lies close to an inner chamber or the  $\mathcal{A}$ -discriminant variety.

The developed program intends to identify triangulations of ALL outer chambers. In order to ensure all outer chambers are triangulated, I have identified unit vectors that lie between rays of the  $\mathcal{A}$ -discriminant variety and are scaled by a factor of 5 to send each unit vector far into its corresponding outer chamber.

**Definition 4.1.** A *ray* is the direction that the  $\mathcal{A}$ -discriminant variety extends to infinity. These points of the parametrization are *infinite singularities* of the  $\mathcal{A}$ -discriminant variety.

Importantly, these rays are defined by the rows of  $-\mathcal{B}$ . Although not useful in practicality to view the chambers separated by the rays as chambers of coefficient space, it can be useful to view all the triangulations in one diagram. It can thus be noted, that adjacent triangulations are separated only by a *bistellar flip*.

**Definition 4.2.** A *bistellar flip* is when a quadrilateral triangulated using one diagonal is switched to be triangulated by the other diagonal.

Figure 5 shows the triangulations of Support  $\mathcal{A} = \begin{bmatrix} 0 & 1 & 0 & 4 & 1 \\ 0 & 0 & 1 & 1 & 4 \end{bmatrix}$ .

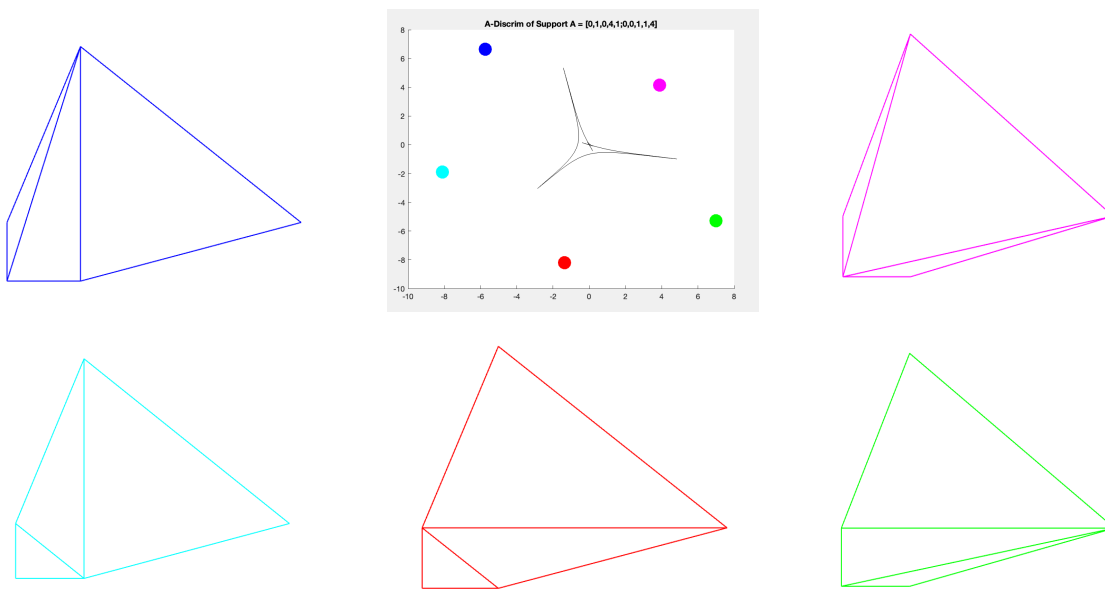


Figure 5: Triangulations within chambers of  $\mathcal{A} = \begin{bmatrix} 0 & 1 & 0 & 4 & 1 \\ 0 & 0 & 1 & 1 & 4 \end{bmatrix}$ .

It is important to note that this method of triangulation using the *Lifted Convex Hull* enables us to triangulate with 5 points even if there exists a point that lies inside of rather than as a vertex of the convex polytope. However, when the convex polytope has fewer than 5 vertices, the resulting triangulation may not involve all points. See Figure 7 for an example of this kind of triangulation.

## 4.2 Viro Diagrams with Triangulated Polytopes

With the triangulated polytope, we now give each vertex a sign based on the signs of the coefficients. There is an additional complication because now there are more edges involved in drawing the Viro Diagram. Again we identify edges with vertices of opposite signs. However, this time we classify these edges as either *outer edges* or *inner edges*. Inner edges extend between non-adjacent vertices and go through the polytope while outer edges are also edges of the convex polytope. For each outer edge, draw an outer normal, centered at the midpoint of the edge.

For each inner edge, draw a segment through the midpoint of this inner edge from the outer edges on either side that have outer normals already. This process is effective for the following reasons. Each triangle only has one inner edge. Inner edges are shared by two adjacent triangles. If a triangle has an inner edge with two opposite signed vertices, then that triangle must have an outer edge with an outer normal.

See Figure 6 for the resulting Viro Diagrams of support  $\mathcal{A} = \begin{bmatrix} 0 & 1 & 0 & 4 & 1 \\ 0 & 0 & 1 & 1 & 4 \end{bmatrix}$  using sign changes  $+ - - + +$ . Reference figures 2 for the actual zero sets of the outer chambers of this signed contour. Notice

that different triangulations may still produce the same isotopy type. This highlights the usefulness of this process because it preserves Proposition 1.1 (isotopy type is preserved throughout a chamber).

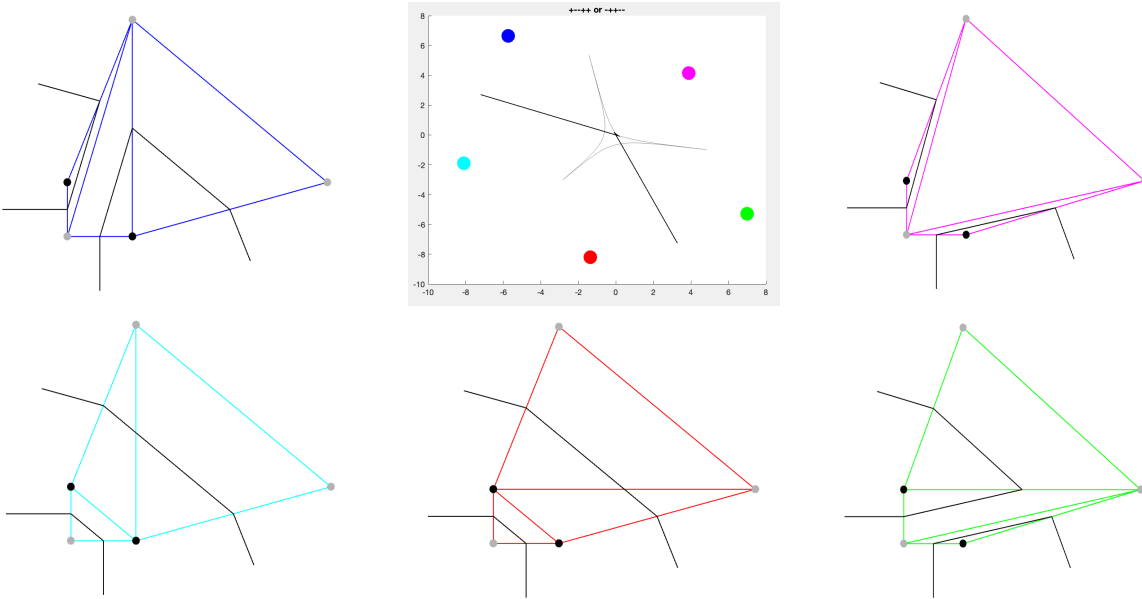


Figure 6: Isotopy Types of signed contour  $+ - - + +$  (or  $- + + - -$ )

See Figure 7 for an example where some exponent vectors are inside of the convex polytope,  $\mathcal{A} = \begin{bmatrix} 0 & 1 & 2 & 1 & 4 \\ 0 & 2 & 1 & 4 & 1 \end{bmatrix}$ , signs =  $+ - + + +$ . There are no inner chambers and it is clear that the signed contour divides the reduced coefficient space into two chambers of different isotopy types.

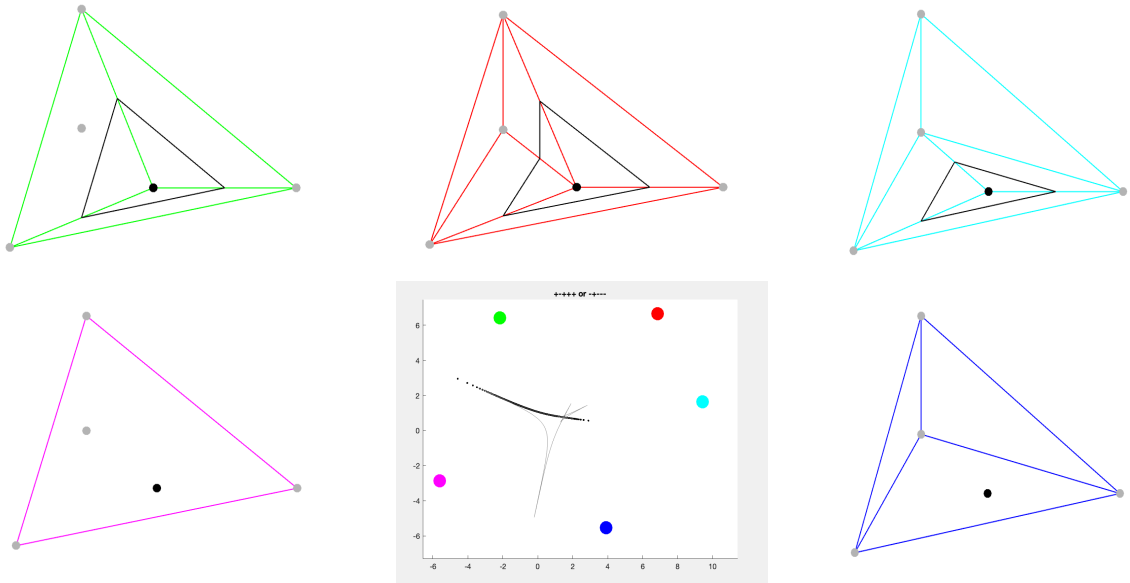


Figure 7: Isotopy types within chambers of Support  $\mathcal{A} = \begin{bmatrix} 0 & 1 & 2 & 1 & 4 \\ 0 & 2 & 1 & 4 & 1 \end{bmatrix}$  with signed contour  $+ - + + +$

This completes the process of determining isotopy types within outer chambers. As a summary, first we determine the triangulations of the outer chambers of the  $\mathcal{A}$ -discriminant variety using the Lifted Convex Hull. These triangulations are the same regardless of the signed contour we are focusing on. To move onto the next step, we must pick a signed contour to focus on. Then, we use the triangulated convex polytope with sign labeled vertices to draw Viro Diagrams, giving the isotopy type of the zero set in various regions.

## 5 Determining Chamber of a Coefficient Vector

The biggest open question in this field of research is working on determining which chamber a coefficient vector lies in. It is visually trivial, but the fact that we have used a parametrization to plot the  $\mathcal{A}$ -discriminant variety complicates this mathematically and algorithmically. We cannot use inequalities to determine chamber. The explicit  $\mathcal{A}$ -discriminant formulas are non-trivial to determine and use, which is what makes the Horn-Kapranov Parametrization so powerful for other aspects of this process.

### 5.1 Transitioning between 2D Points and Coefficient Vectors

To plot the coefficient vectors of pentanomials we use the formula  $\log |c| \cdot \mathcal{B}$ .

To find the absolute value of a coefficient vector that maps to a point in the 2D space, we use the following process. Let  $p = [p1, p2]$  be the point in 2D space. Then let  $\alpha \cdot p = \mathcal{B} \cdot \mathcal{B}^T$ . Then  $c = e^{\alpha \cdot \mathcal{B}^T}$ .

This is the process that was used to plot points in various chambers, but knowing the 2D coordinate does not tell us which side of a signed contour.

### 5.2 Previous Research on Sidedness

**Definition 5.1.** *Sidedness* is the property of a given coefficient vector  $c$  that identifies which side of a signed contour  $c$  exists on.

Previous research has identified a process of approximating signed contours using its rays. The idea is to use Horn Kapranov Parametrization with a  $3 \times 2$  null basis  $\mathcal{B} = \begin{bmatrix} -ray_{1,1} & -ray_{1,2} \\ -ray_{2,1} & -ray_{2,2} \\ (ray_{1,1} + ray_{2,1}) & (ray_{1,2} + ray_{2,2}) \end{bmatrix}$ .

Following this parametrization, we shift the parametrization so that it not only has the correct concavity and shape but also occurs in the correct location.

This approximation is highly effective on most signed contours, but whenever there is a cusp in the signed contour, this approximation fails. See figure 8 for an example using Support  $\mathcal{A} = \begin{bmatrix} 0 & 1 & 2 & 1 & 4 \\ 0 & 2 & 1 & 4 & 1 \end{bmatrix}$  which has two signed contours with one cusp each.

Since we have identified a process of identifying the number and locations of cusps within the true parametrization, we can use this to figure out which signed contours this  $3 \times 2$  approximation will work for.

Naturally, the next logical step is to figure out a better approximation for signed contours with cusps.

### 5.3 Approximations for Signed Contours with One Cusp

I tried two ideas to approximate the signed contours with one cusp. The first was to use a piecewise approximation using two distinct  $3 \times 2$  Approximations. The second was to map a simpler  $\mathcal{A}$ -discriminant that contains a cusp onto our cusp. The  $\mathcal{A}$ -discriminant of cubic (Support =  $[0, 1, 2, 3]$ ) has a cusp. Solving for sidedness of the cubic  $\mathcal{A}$ -discriminant (not parametrization) is better than solving the explicit formula of the  $\mathcal{A}$ -discriminant variety for supports with higher degrees.





Figure 8:  $3 \times 2$  Approximations in Green with Actual in Blue

### 5.3.1 Piece-wise Approximation using Two $3 \times 2$ Parts

Rather than using the two rays of the signed contour to form one  $(3 \times 2)$   $\mathcal{B}$ , I created two parametrized approximations,  $\mathcal{B}_1, \mathcal{B}_2$ , each using one of the rays and then using the cusp as the second input.

Let  $ray_1 = (ray_{1,1}, ray_{1,2})$  and  $ray_2 = (ray_{2,1}, ray_{2,2})$  be the two directions that the signed contour extends to infinity in. Let  $u = (u_1, u_2)$  be the coordinates of the cusp and  $\lambda_u$  be 'when' the cusp occurs.

**Proposition 5.1.** If the  $\mathcal{B}$  of the parametrized signed contour is orthonormal, the coordinates of each point of the parametrizations give vector for the normal to the curve at that location.

By Proposition 5.1,  $u$  also gives the normal vector to each curve as it approaches the cusp.

$$\text{Let } \mathcal{B}_1 = \begin{bmatrix} -ray_{1,1} & -ray_{1,2} \\ -u_1 & -u_2 \\ (ray_{1,1} + u_1) & (ray_{1,2} + u_2) \end{bmatrix} \text{ and let } \mathcal{B}_2 = \begin{bmatrix} -u_1 & -u_2 \\ -ray_{2,1} & -ray_{2,2} \\ (u_1 + ray_{2,1}) & (u_2 + ray_{2,2}) \end{bmatrix}.$$

Like the previous research on using  $3 \times 2$  approximations, we must shift each approximation onto the region where the cusp is. Thus the resulting approximation is given by  $\log |\lambda \cdot \mathcal{B}^T| \cdot \mathcal{B}$ , where  $\mathcal{B} = \begin{cases} \mathcal{B}_1, & \text{if } \lambda < \lambda_u \\ \mathcal{B}_2, & \text{if } \lambda > \lambda_u \end{cases}$

Figure 9 depicts the resulting approximation for the two cusps shown in figure 8.

These approximations allow the cusp to line up, but they do slightly distort the directions as the curve goes to infinity. More research can be done on tweaking these approximations to improve this aspect.

### 5.3.2 Mapping Cubic Cusp

The difficulty of process for finding the Horn-Kapranov Paramtrization for any support is comparable. However, the difficulty of explicitly solving the original  $\mathcal{A}$ -discriminant formula differs from support to support. There are many  $\mathcal{A}$ -discriminant varieties that contain cusps, with formulas of various difficulty.

The simplest support that contains a signed contour with one cusp is given by the cubic function, support  $\mathcal{A} = \begin{bmatrix} 0 & 1 & 2 & 3 \end{bmatrix}$ . The goal of this second approximation is to find an algorithm that maps the cusp

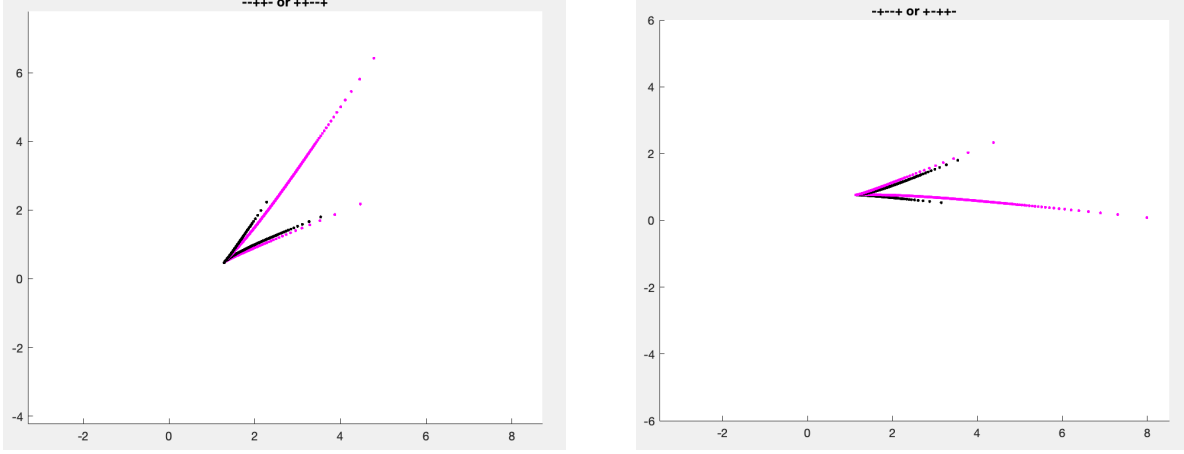


Figure 9: Piecewise Approximations

found in the cubic  $\mathcal{A}$ -discriminant variety onto any other signed contour with one cusp. Let  $S_0$  be the signed contour we are trying to approximate.

With some pre-processing, I determined which signed contour of the cubic contained the cusp. Let this signed contour be  $S_1$ . One aspect of the Horn-Kapranov Parametrization that becomes useful here is the flexibility of the  $\mathcal{B}$  matrix. There are many different vectors that can form the basis for the right nullspace of  $\mathcal{A}$ . Different  $\mathcal{B}$  matrices will rotate the  $\mathcal{A}$ -discriminant variety around. We can think about these differences as different angles and orientations of slicing the higher dimension space down to the 2D reduced  $\mathcal{A}$ -discriminant space.

The idea here is to find the  $\mathcal{B}$  that sent the rays of  $S$  in the desired directions (i.e. the rays of  $S_0$ ). This can be achieved by setting the first row of  $\mathcal{B}$  equal to  $-ray_1$  and the last row of  $\mathcal{B}$  equal to  $-ray_2$ . This is effective because the first and last rows of  $\mathcal{B}$  specify the information of  $S_1$ .

To solve for the remaining rows that form a right nullspace, I did as follows:

$$\begin{bmatrix} 1 & 1 & 1 & 1 \\ 0 & 1 & 2 & 3 \end{bmatrix} \cdot \begin{bmatrix} -ray_{1,1} & -ray_{1,2} \\ a & b \\ c & d \\ -ray_{2,1} & -ray_{2,2} \end{bmatrix} = \begin{bmatrix} 0 & 0 \\ 0 & 0 \end{bmatrix}.$$

$$\begin{bmatrix} a + c - ray_{1,1} - ray_{2,1} & b + d - ray_{1,2} - ray_{2,2} \\ a + 2c - 3ray_{2,1} & b + 2d - 3ray_{2,2} \end{bmatrix} = \begin{bmatrix} 0 & 0 \\ 0 & 0 \end{bmatrix}.$$

The resulting equations are

$$\begin{aligned} a + c &= ray_{1,1} + ray_{2,1}, & b + d &= ray_{1,2} + ray_{2,2}, \\ a + 2c &= 3ray_{2,1}, & b + 2d &= 3ray_{2,2}. \end{aligned}$$

$$\mathcal{B} = \begin{bmatrix} ray_{1,1} & ray_{1,2} \\ 2ray_{1,1} - ray_{2,1} & 2ray_{1,2} - ray_{2,2} \\ 2ray_{2,1} - ray_{1,1} & 2ray_{2,2} - ray_{1,2} \\ ray_{2,1} & ray_{2,2} \end{bmatrix}.$$

This  $\mathcal{B}$  orients the cubic cusp in the correct directions but does not necessarily align the cusps together. the shifting technique used in  $3 \times 2$  matrix approximations is no longer effective because the  $S_1$  does not begin at the cusp, nor is its shape and orientation directed by the cusp. Noticing that the found  $\mathcal{B}$  has vectors that are larger than unit vectors, I decided to scale  $\mathcal{B}$  down. Unfortunately, in scaling  $\mathcal{B}$ , there is less precision as we move out to infinity. This creates a tradeoff between precision at the cusp and precision

at infinity. More research needs to be done at determining the optimal scaling for  $\mathcal{B}$  that maximizes the precision in both these areas.

Figure 10 shows examples of scaling using  $\frac{\mathcal{B}}{8\|(2ray_{1,1}-ray_{2,1}, 2ray_{1,2}-ray_{2,2})\|}$ .

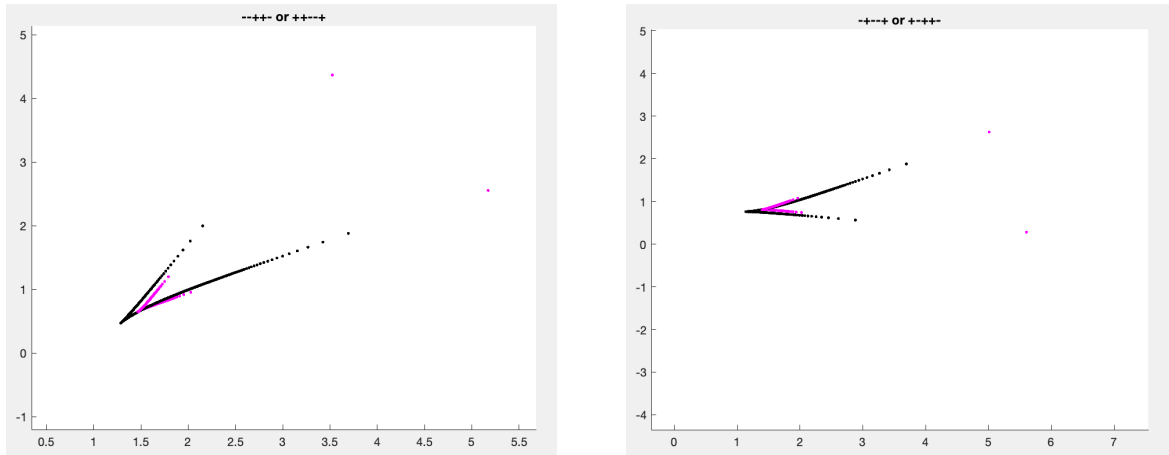


Figure 10: Cubic Cusp Approximations

## 6 Conclusion

This paper presents the development of a new tool in MATLAB that draws isotopy types of outer chambers of  $\mathcal{A}$ -discriminants of  $n = 2$  near circuits. It also presents some new findings on approximating signed contours that contain one cusp. These approximations are part of the larger goal of improving the ability to determine sidedness of coefficient vectors for near-circuits polynomials. Future research can continue working on improving approximations for sidedness and also developing isotopic models for inner chambers.

## Acknowledgements

I want to acknowledge that many of the ideas discussed in Sections 5.2 and 5.3 came from unpublished research done by Ellen Chlachidze during 2022.

I want to thank Dr. Maurice Rojas for his mentorship during the 2023 Texas A&M Mathematics REU in Algorithmic Algebraic Geometry, Weixun Deng for his guidance, and the NSF for funding this research.

I also want to thank all those who have supported my math journey so far, including my family, professors at Bowdoin College, and teachers from middle and high school. During the inevitable setbacks of research, I found myself persevering because of those who have lifted me up and believed in me.

## References

- [FNR17] Jens Forsgård, Mounir Nisse, and J. Maurice Rojas. New subexponential fewnomial hypersurface bounds, 2017.
- [Har80] Robert M. Hardt. Semi-algebraic local-triviality in semi-algebraic mappings, Apr 1980.
- [Kap91] M.M. Kapranov. A chracterization of a-discriminantal hypersurfaces in terms of the logarithmic gauss map. *Mathematische Annalen*, 290(2):277–286, 1991.
- [Mil69] John Milnor. Morse theory. *Annals of Mathematics studies*, (51), 1969.
- [RR17] J. Maurice Rojas and Korben Rusek. A-discriminants for complex exponents, and counting real isotopy types, 2017.
- [Vir00] Oleg Viro. Dequantization of real algebraic geometry on logarithmic paper, 2000.

*E-mail Address:* vmiriyagalla@bowdoin.edu